Preprints.org

Article

Not peer-reviewed version

# Thymol@activated Carbon Nanohybrid for Low-Density Polyeth-Ylene Based Active Packaging Films for Pork Fillets Shelf-Life Extension

Aris E. Giannakas *, Vassilios K. Karabagias, Dimitrios Moschovas, Areti Leontiou, Ioannis K. Karabagias, Stavros Georgopoulos, Andreas Karydis-Messinis, Konstantinos Zaharioudakis, Nikolaos Andritsos, George Kehayias, Apostolos Avgeropoulos, Charalampos Proestos, Constantinos E Salmas *

Posted Date: 7 June 2023

doi: 10.20944/preprints202306.0500.v1

Keywords: activated carbon; thymol; low-density polyethylene; active packaging; control release; kinetics; pork fillets; heme iron; shelf life

Preprints.org is a free multidiscipline platform providing preprint service that is dedicated to making early versions of research outputs permanently available and citable. Preprints posted at Preprints.org appear in Web of Science, Crossref, Google Scholar, Scilit, Europe PMC.

Copyright: This is an open access article distributed under the Creative Commons Attribution License which permits unrestricted use, distribution, and reproduction in any medium, provided the original work is properly cited.

Preprints.org (www.preprints.org) | NOT PEER-REVIEWED | Posted: 7 June 2023 doi:10.20944/preprints202306.0500.v1

Disclaimer/Publisher's Note: The statements, opinions, and data contained in all publications are solely those of the individual author(s) and contributor(s) and not of MDPI and/or the editor(s). MDPI and/or the editor(s) disclaim responsibility for any injury to people or property resulting from any ideas, methods, instructions, or products referred to in the content.

*Article*

# Thymol@activated Carbon Nanohybrid for Low-Density Polyethylene Based Active Packaging Films for Pork Fillets Shelf-Life Extension

**Aris E. Giannakas [1,*], Vassilios K. Karabagias [1], Dimitrios Moschovas [2], Areti Leontiou [1], Ioannis K. Karabagias [1], Stavros Georgopoulos [1], Andreas Karydis-Messinis [2], Konstantinos, Zaharioudakis [1], Nikolaos Andritsos [1], George Kehayias [1], Apostolos Avgeropoulos [2], Charalampos Proestos [3] and Constantinos E. Salmas [2,*]**

[1] Department of Food Science and Technology, University of Patras, 30100 Agrinio, Greece; vkarampagias@upatras.gr (V.K.K); ikaraba@upatras.gr (I.K.K.); sgeorgop@upatras.gr (S.G.); aleontiu@upatras.gr (A.L.); zacharioudakis.k@upatras.gr (K.Z.)

[2] Department of Material Science and Engineering, University of Ioannina, 45110 Ioannina, Greece; dmoschov@uoi.gr (D.M.); aavger@uoi.gr (A.A)

[3] Laboratory of Food Chemistry, Department of Chemistry, National and Kapodistrian University of Athens Zografou, 15771 Athens, Greece

* Correspondence: agiannakas@upatras.gr (A.E.G.); ksalmas@uoi.gr (C.E.S.)

**Abstract:** Nowadays, bioeconomy and nanotechnology trends push food packaging sector in the replacement of food additives by biobased antioxidant/antibacterial compounds and their inclusion in nanocarriers to control their release. Herein by following this trend, a rich in thymol-(TO) activated carbon (AC) nanostructure (TO@AC) was prepared and physiochemically characterized with various technics. This TO@AC nanostructure as well as pure AC were extruded with low density polyethylene (LDPE) to develop novel active packaging LDPE/TO@AC and LDPE/AC films. X-ray diffractometry, Fourier Transform Infrared Spectroscopy and Scanning Electron Microscopy measuraments shown high dispersity and capability of both AC and TO@AC in LDPE matrix which was resulted in enhanced tensile and water/oxygen barrier properties of obtained LDPE/AC and LDPE/TO@AC films. LDPE/TO@AC films shown higher elongation at break values and water/oxygen barrier than LDPE/AC films and significant antioxidant activity. TO release kinetics studies shown that by increasing TO@AC content the total TO amount released increased and the constant release rate decreased. Pork fillets wrapped with the optimum active film containing 15 wt.% TO@AC and succeed to prevent lipid oxidation and heme iron loss during storage. Estimation of microbial population of pork fillets shown that this active film could extend the microbiological shelf-life of pork fillets by 2 days.

**Keywords:** activated carbon; thymol; low-density polyethylene; active packaging; control release; kinetics; pork fillets; heme iron; shelf life

## 1. Introduction

Nowadays, the need to enhance food safety and shelf-life is driving research and development (R&D) in food technology towards investigating packaging that can not only protect food, but also react with it to preserve, enhance its safety, and extend its shelf-life [1]. This type of packaging is called "active food packaging" [1–3]. Moreover, one of the most recent trends in active food packaging is the removal of food additives from the food itself and their incorporation into the active packaging, and controlling the release of such food additives into the food [4,5]. Along these lines, it is also suggested to replace food additives with natural, abundant chemical compounds that have demonstrated antioxidant and antibacterial activity [4]. These bioactive antioxidant/antibacterial compounds are essential oils (EOs) and their components which are mainly monoterpenes, sesquiterpenes, alcohols, phenols, aldehydes, ketones, and esters [6–8]. Over the past few years, considerable effort has been devoted to developing polymers or biopolymers-based active packaging films incorporated with various essential oils such as oregano oil [9,10], thyme oil [9–11], basil oil

© 2023 by the author(s). Distributed under a Creative Commons CC BY license.

Preprints.org (www.preprints.org) | NOT PEER-REVIEWED | Posted: 7 June 2023 doi:10.20944/preprints202306.0500.v1



[12,13], orange oil [14], lemongrass oil [15] or their derivatives such as thymol[16], carvacrol [17], cinnamaldehyde [18] and limonene [19]. The main disadvantage of directly incorporating EOs into the polymer or biopolymer matrix is that their volatile nature leads to rapid loss, thereby deactivating the active properties of the packaging. To address this, it has been proposed to adsorb these EOs or their derivatives onto inexpensive, naturally abundant materials such as nanoclays before integrating the resulting EOs/nanoclay hybrid structure into the polymer or biopolymer matrix [20]. This approach enables the development of polymers or biopolymers/EOs/nanoclays active packaging films with enhanced mechanical, tensile, water/oxygen barrier properties, and controlled release of antioxidant and antibacterial properties [21–23]. As such, nanoclays such as montmorillonite (MMT) and halloysite nanotubes (HNT) have been extensively studied as EOs nanocarriers in the development of polymers or biopolymers/EOs/nanoclays active packaging films [24,25]. More recently, well-known adsorbent multifunctional materials such as natural zeolite (NZ) [26–28], silica-based materials (MCM and SBA-15) [29,30] and carbon-based materials (activated carbon-AC) [31–33] have been suggested as EOs and their derivatives nanocarriers. These materials have an advantage over nanoclays due to their larger specific surface areas and their ability to adsorb and be loaded with higher amounts of EOs or their derivatives. Among various carbon-based nanomaterials, activated carbon (AC) has the advantage of low cost, non-toxicity, and degradability [31]. The effectiveness of AC strongly depends on its pore structure and surface chemistry [31]. AC is used in packaging films because of its adsorption and release capabilities. Thus, it can be used as an adsorbent to remove gases from packaged food or as a nanocarrier for bioactive compounds to be released into food [33,34].

Low-density polyethylene (LDPE) is one of the most used materials for flexible food packaging. Although it is a polymer produced via petrochemistry processes, it could be considered biobased in the future if it will be produced only via the bioethanol process. It has satisfactory strength-at-break properties up to -60 $^{o}$C, good water barrier properties, but high permeability to oxygen, which makes it unsuitable as packaging material for foods sensitive to oxidation deterioration, such as meat products. Oxidative deterioration is the most critical factor following microbial deterioration for pork degradation and the end of its shelf-life [35]. Therefore, it is essential to modify LDPE by enhancing its oxygen barrier properties through the development of an LDPE-based active packaging material. This could be more valuable if the modification follows circular economy trends, which propose the use of biobased raw materials such as EOs and AC. Recently, Macca carbon (MC) powder, a biomass derived from macadamia nut, was incorporated into LDPE by melt-compounding and subsequent melt-extrusion operations [36]. The obtained LDPE/MC films were characterized physically with optical microscopy, scanning electron microscopy (SEM), differential scanning calorimetry (DSC), thermal gravimetric analysis (TGA), while the mechanical, water/oxygen barrier, transmission, and antimicrobial properties were also studied [36]. The weight percent content of MC powder in LDPE varied from 0.5% up to 5%.

In recent studies, a "green" method was reported for the extraction of a thymol-rich (TO) fraction from thyme oil and its subsequent adsorption on halloysite nanotubes (HNT) and natural zeolite (NZ) to create innovative TO@HNT and TO@NZ nanohybrids [37,38] These nanohybrids were recently incorporated into low-density polyethylene (LDPE) to develop promising active packaging films, LDPE/TO@HNT and LDPE/TO@NZ, aimed at preserving low-fat pork fillets [39,40]. In this study, the same green method is employed to adsorb TO onto activated carbon (AC), resulting in the TO@AC nanohybrid. The obtained TO@AC was characterized physiochemically through XRD analysis, FTIR spectroscopy, as well as TG and DSC experiments. Subsequently, the TO@AC nanohybrid was integrated into the LDPE matrix at 5, 10, and 15 wt.% contents using an extrusion molding process to create LDPE/5TO@AC, LDPE/10TO@AC, and LDPE/15TO@AC active packaging films. For comparison, LDPE films with 5, 10, and 15 wt.% AC content, without TO, were prepared. Both LDPE/AC and LDPE/TO@AC films were characterized physiochemically with XRD analysis, FTIR spectroscopy, SEM imaging, and DSC experiments. The tensile properties, water/oxygen barrier properties, and total antioxidant activity of the films were also examined. In advance, the kinetics of TO release were studied for all active LDPE/TO@AC films. The objective of these characterizations

Preprints.org (www.preprints.org) | NOT PEER-REVIEWED | Posted: 7 June 2023 doi:10.20944/preprints202306.0500.v1



and property investigations was to identify the most promising LDPE/TO@AC active film. The LDPE/TO@AC film with the best packaging properties, as well as LDPE/AC and pure LDPE films, were utilized to wrap pork fillets, and their shelf-life was evaluated by measuring their lipid oxidation through the TBARs method, their heme iron values, and the total bacterial count values. The unique innovations of this work can be summarized as follows: (i) the development and characterization of novel TO@AC nanohybrids, to the best of our knowledge, for the first time; (ii) the incorporation of pure AC and modified TO@AC nanohybrids into LDPE at high contents of 5, 10, and 15 wt.%; (iii) the development, characterization, and use of novel LDPE/TO@AC active packaging films for pork fillet preservation, to the best of our knowledge, for the first time; and (iv) in alignment with recent works [39,40] the identification of a direct linear relationship between TBARs lipid oxidation values and heme iron values of pork fillets. Moreover, the microbiological population, as estimated by total variable counts, indicated a shelf-life extension of 2 days for pork fillets.

## 2. Materials and Methods

### *2.1. Materials*

Thyme oil used was supplied by Chemco (Via Achille Grandi, 13 - 13/A, 42030 Vezzano sul Crostolo RE, Italy). LDPE (CAS No. 9002-88-4) with density 0.925 g $cm^{-3}$ and melting point 116 °C was supplied by Sigma-Aldrich (Sigma-Aldrich, St. Louis, MO, USA). Fresh pork fillets "skalopini" type was a kind offering of Aifantis Company (Aifantis Group – Head Quarters, Acheloos Bridge, Agrinio, Greece 30100). Three fresh and deboned pork fillets "skalopini type" with approximate weight 700 g each were provided by a local meat processing plant Aifantis Company within one hour after the slaughter. Activated carbon (AC) from spent coffee of students café of University of Ioannina was prepared with a pyrolysis process and a treatment with KOH according to previous report [41]. The Brünaüer–Emmett–Teller surface area of AC was to 1372 $m^2/g$ and the micropore volume was 84.6% [41].

### *2.2. Preparation of TO@AC Nanohybrid*

The process of modifying pure AC with a TO-rich fraction was the same as the process used for the modification of HNT and NZ, as described recently [37,38]. As illustrated in Figure 1, the process was carried out in two steps. In the first step, a distillation took place using a distillation apparatus on pure thyme oil at 200 °C to obtain a TO-rich fraction and separate the most volatile limonene-cymene fraction. In the second step, TO adsorption on AC occurred by placing an AC bed above the spherical glass container containing the TO-rich fraction and evaporating the TO-rich fraction by heating it to 250 °C. Thus, the TO@AC nanohybrid was obtained and kept for further physicochemical characterization.

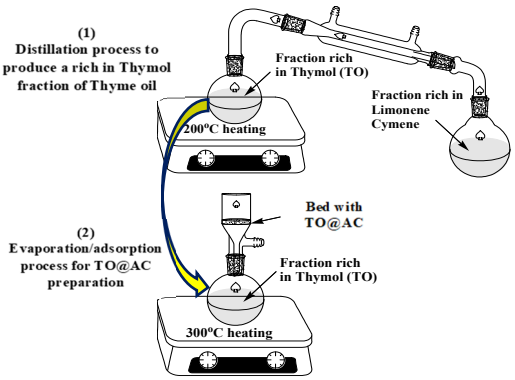


**Figure 1.** Schematic presentation of process used for TO@AC nanohybrids preparation.

Preprints.org (www.preprints.org) | NOT PEER-REVIEWED | Posted: 7 June 2023 doi:10.20944/preprints202306.0500.v1



*2.3. Preparation of LDPE/AC and LDPE/TO@AC Films*

The preparation of LDPE/AC and LDPE/TO@AC films was accomplished using a mini lab twin screw extruder (Haake Mini Lab II, ThermoScientific, ANTISEL, S.A., Athens, Greece), operated at 140 °C and 100 rpm for 3 minutes [21]. LDPE pellets were mixed with pure AC and the previously prepared TO@AC powder to achieve nominal AC and TO@AC weight percentages of 5, 10, and 15% (refer to Figure 2). The resultant samples were labeled as LDPE/5AC, LDPE/10AC, LDPE/15AC, LDPE/5TO@AC, LDPE/10TO@AC, and LDPE/15TO@AC. A pure LDPE sample was also prepared for comparison. Following the extrusion process, the LDPE/AC and LDPE/TO@AC samples, as well as the pure LDPE, were thermomechanically transformed into films (see Figure 2). This transformation was achieved by operating a hydraulic press with heated platens at 110 °C and a constant pressure of 2 MPa for 2 minutes [12,42].

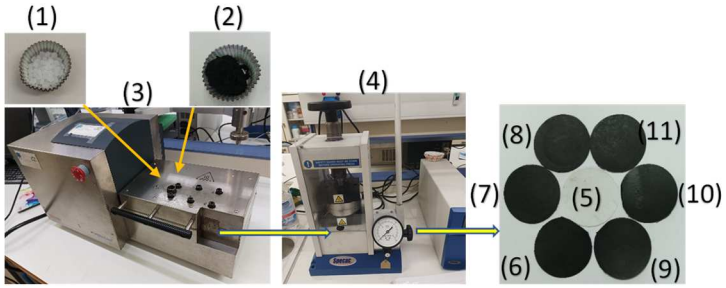


**Figure 2.** Schematic representation of the extrusion process for the preparation of LDPE/AC and LDPE/TO@AC films. (1) LDPE pellets, (2) TO@AC powder, (3) mini lab twin screw extruder, (4) Lab hydravlic press with heated platens, (5) LDPE film, (6) LDPE/5AC film, (7) LDPE/10AC film, (8) LDPE/15AC film, (9) LDPE/5TO@AC film, (10) LDPE/10TO@AC film and (11) LDPE/15TO@AC film.

*2.4. Physicochemical Characterization of AC, TO@AC, Powders and LDPE/AC and LDPE/TO@AC Films*

To ascertain potential alterations in the crystallinity of AC during the process of TO@AC nanohybrid formation, XRD analyses were performed on both pure AC and TO@AC. The crystal structure of the resulting LDPE/AC, LDPE/TO@AC films, and the pure LDPE film were also examined via XRD analyses. All XRD measurements were conducted using a Brucker XRD D8 Advance diffractometer (Brüker, Analytical Instruments, S.A., Athens, Greece) with a LINXEYE XE high-resolution energy dispersive detector, under experimental conditions set in accordance with previous reports. Probable interactions between AC and the adsorbed TO molecules were explored through FTIR spectroscopy measurements on pure AC and the modified TO@AC nanohybrids. Additionally, the interactions between AC, TO@AC, and the LDPE matrix were investigated with FTIR spectroscopy measurements on the pure LDPE film and all LDPE/AC and LDPE/TO@AC films. The FTIR measurements employed an FT/IR-6000 JASCO Fourier transform spectrometer (JASCO, Interlab, S.A., Athens, Greece). Differential Scanning Calorimetry (DSC) measurements were conducted on pure AC and modified TO@AC nanohybrids using a DSC214 Polyma Differential Scanning Calorimeter (NETZSCH manufacturer, Selb, Germany). The total amount of TO fraction adsorbed onto AC was determined through Thermogravimetric Analysis (TGA) experiments performed on pure AC and the modified TO@AC nanohybrid, utilizing a Perkin-Elmer Pyris Diamond TGA/DTA instrument (Interlab, S.A., Athens, Greece). Lastly, the surface and cross-sectional morphology of all resulting LDPE/AC and LDPE/TO@AC films, as well as the pure LDPE film, were scrutinized via SEM analysis with an accompanying EDX analysis. This process employed a JEOL JSM-6510 LV SEM Microscope (Ltd., Tokyo, Japan) equipped with an X-Act EDS-detector from Oxford Instruments, Abingdon, Oxfordshire, UK (an acceleration voltage of 20 kV).

Preprints.org (www.preprints.org) | NOT PEER-REVIEWED | Posted: 7 June 2023 doi:10.20944/preprints202306.0500.v1



*2.5. Tensile Measurements of LDPE/AC and LDPE/TO@AC Films*

For all obtained LDPE/AC and LDPE/TO@AC films as well as for pure LDPE film tensile properties were measured according to according to the ASTM D638 method using a Simantzü AX-G 5kNt instrument (Simantzu. Asteriadis, S.A., Athens, Greece) following the methdology described previously [21,39,43].

*2.6. Water Vapor Transmittion Rate (WVTR) and Water Diffusion Coefficient ($D_{wv}$)*

WVTR values for all obtained LDPE/AC and LDPE/TO@AC films as well as for pure LDPE film were measured with a handmade apparatus according to ASTM E96/E 96M-05 method [42,44]. From WVTR values the water vapor diffusion coefficient values ($D_{wv}$) were calculated according to the methodology descibed in detail recently [43,45].

*2.7. Oxygen Transmittion Rate Values (O.T.R.) and Oxygen Diffusion Coeficient ($P_{O2}$)*

For all obtained LDPE/AC and LDPE/TO@AC films as well as for pure LDPE film O.T.R. values were measured by using an oxygen permeation analyzer (O.P.A., 8001, Systech Illinois Instruments Co., Johnsburg, IL, USA) according to the ASTM D 3985 method (23 $^{o}$C and 0% RH). From these values oxygen diffusion coeficient ($P_{O2}$) values were obtained by following the methodology descriped in detail recently [43,45].

*2.8. Total Antioxidant Activity of Films*

The antioxidant activity of all obtained films measured according to 2,2-diphenyl-1-picrylhydrazyl radical (DPPH) assay. In 4 ml of 30 ppm DPPH ethanolic solution approximately 5 mg of LDPE/5TO@AC, LDPE/10TO@AC, and LDPE/15TO@AC film were added and the adsorbance at 517 nm was recorded as a function of time for 1 h (60min), 2 h (120min), 3 h (180), 1day (1440) and 2 days (2880 min). As a blank sample the absorbance of 4 ml of 30ppm DPPH ethanolic solution without the addition of any film was recorded as a function of time too. The % antioxidant activity calculated by using the next equation (1):

$$\textbf{\% film antioxidant activity} = [(A_{t,film} - A_{t,blank})/A_0] \times 100 \quad (1)$$

where $A_{t,film}$ is the absorbance of each film as a function of time, $A_{t,blank}$ the absorbance of blank sample as a function of time and $A_0$ the initital absorbance of each sample solution.

*2.9. TO Release Test - Calculation of Released to wt.% Content and TO Released Diffusion Coefficient ($D_{TO}$)*

For all LDPE/TO@AC films the released TO experiments a moisture analyzer AXIS AS-60 (AXIS Sp. z o.o. ul. Kartuska 375b, 80-125 Gdańsk) was employed according to the methodology described previously [40]. Approxiamtely 300 to 500 mg of each film used for the control release experiments. The diffusion coefficient ($D_{TO}$) for TO release out of the obtained LDPE/xTO@AC films process, was calculated according to the following equation (2):

$$\frac{m_t}{m_\infty} = \sqrt{4\frac{D.t}{\pi.l^2}} \quad (2)$$

where $m_t$ and $m_\infty$ is the amount of TO released form the film after time t and after equilibrium time $t_{eq} \rightarrow \infty$ respectivelly, D is the diffusion coefficient, and *l* is the average film thickness.

The linearization of equation (6) is leading to the slightly modified equation (3):

$$\left(\frac{m_t}{m_\infty}\right)^2 = 4\frac{D \times t}{\pi \times \ell^2} \quad (3)$$

By employing the pseudo-second order sorption mechanism model [41] we calculated the desorption rate Constant $K_2$ and the maximum TO desorbed amount $q_e$ according to the equation:

Preprints.org (www.preprints.org) | NOT PEER-REVIEWED | Posted: 7 June 2023 doi:10.20944/preprints202306.0500.v1



$$q_t = \frac{q_e^2 \times k_2 \times t}{q_e \times k_2 \times t + 1} \quad (3)$$

where $q_t = m_t/m_0$ and $q_e = 1$.

*2.10. Packaging Preservation Test of "Skaloppini Type" Fresh Pork Meat Fillets*

The pork fillets were wraped aseptically between two LDPE@15TO@AC active films with a diameter of 11 cm (see Figure 3). For comparison pork fillets wrapped also with two LDPE/15AC films and two pure LDPE films (control sample) (see Figure 3). All the as wrapped pork fillets were folded inside the packaging paper of the local meat processing plant Aifantis, without the inner membrane-used by the company for packaging. After packaging, the fillets were placed in a preservation chamber at 4±1°C and then measured for lipid oxidation and heme iron content.

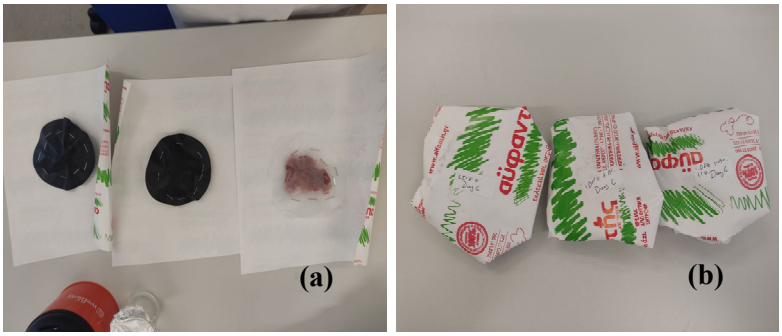


**Figure 3.** (a) Wrapping of fresh pork fillets inside two LDPE@15TO@AC, LDPE/15AC and pure LDPE films, (b) folding of wrapped pork fillets inside the packaging paper of Aifantis company.

*2.11. Packaging Test of Fresh Pork Fillets*

2.11.1. Lipid Oxidation of Pork Fillets with Thiobarbituric Acid Reactive Substances

Thiobarbituric acid reactive substances (TBARS) values of packed pork fillets after 2, 4, 6, 8, 10 and 12 days were determined with the method of Tarladgis et. al. [46] as it was recently modified by Karabagias et al. [47]. The methodology for determination of the TBARS values of packaged fresh pork fillets described in detail recently [39,40].

Heme Iron Content

The heme iron content of packaged fresh pork fillets was determined according to the method reported by Clark et al. [48] as it is desribed in deatail recently [39,40].

Total Variable Counts (TVC) of Pork Fillets

TVC was monitored with respect to storage time. Ten grams of pork fillets were removed aseptically from each packaging treatment using a spoon, transferred to a stomacher bag (Seward Medical, Worthing, West Sussex, UK), containing 90 mL of sterile buffered peptone water (BPW, NCM0015A, Heywood, BL97JJ, UK) (0.1g/100mL of distilled water) and homogenized using a stomacher (LAB Blender 400, Seward Medical, UK) for 90 s at room temperature. For the microbial enumeration, 0.1 mL of serial dilutions (1:10 diluents, buffered peptone water) of pork meat homogenates was spread on the surface of plate count agar (PCA, NCM0010A, Heywood UK). TVC was determined using after incubation for 2 days at 30 ºC [49].

*2.12. Statstical Analysis*

In this study, an extensive array of tests were conducted on a minimum of three separate samples. These tests encompassed an assessment of structural, mechanical, and barrier properties, alongside a range of others, including antioxidant activities, controlled release, TBARS, heme iron,

Preprints.org (www.preprints.org) | NOT PEER-REVIEWED | Posted: 7 June 2023 doi:10.20944/preprints202306.0500.v1



and TVC tests. The results presented in the tables throughout this work are averages derived from these measurements, with each table also displaying the standard deviation. Hypothesis testing was performed to evaluate the equality of means. IBM's SPSS Statistics software, version 20, was used to perform the necessary statistical analysis. This involved implementing the ANOVA method, setting confidence intervals at 95% and the significance level at $p = 0.05$. In addition, the assurance of mean equality (EA%) or inequality (IA%) was examined based on empirical equations previously outlined in literature [50]. Across all tests, it was observed that the mean values of the various sample properties significantly differed, all with an assurance factor exceeding 52%.

## 3. Results and Discussion

### *3.1. Physicochemical Characterization of AC and TO@AC Nanohybrid*

The XRD plot of pure AC powder (depicted as line (1) in Figure 4a) is consistent with a typical amorphous material. After the adsorption of TO to create the TO@AC modified nanohybrid, a broad peak appears at around 18° 2theta in the XRD plot (see line (2) in Figure 4a), suggesting that the adsorption of TO has subtly influenced the amorphous structure of pure AC. The line (1) in the FTIR graph (Figure 4b) corresponds to the FTIR plot of pure thyme oil. The bands observable at 3530 to 3433 $cm^{-1}$ are attributed to the stretching vibration of O-H groups. The bands around 3100–3000 $cm^{-1}$ are ascribed to the stretching vibrations of aromatic and alkenic groups of TO molecules. The bands at 2958 and at 2868 $cm^{-1}$ pertain to the stretching mode of C-H groups. The bands between 1500 $cm^{-1}$ and 1300 $cm^{-1}$ are ascribed to the bending of C-H on the C-O-H group and the bending of aliphatic $CH_2$ groups [37,39,51]. The FTIR spectra of pure AC (see line (2) in Figure 4b) prominently display bands at 1590 $cm^{-1}$ and 1260 $cm^{-1}$. The band at 1590 $cm^{-1}$ corresponds to the stretching vibration modes of carbonylic (-COO-) groups, while the band at 1260 $cm^{-1}$ is assigned to the stretching vibration of C-O groups [41]. The band with a maximum at approximately 3420–3440 $cm^{-1}$ is attributed to the O–H stretching mode of hydroxyl groups of the adsorbed water molecules [52]. In the FTIR plot of the modified TO@AC nanohybrid (line (3) in Figure 4b), it is evident that besides the bands of the pure AC, the characteristic bands of TO also exist in the ranges of 2800-3100 $cm^{-1}$, 1300-1500 $cm^{-1}$, and 500-1000 $cm^{-1}$ [37,39,51]. This observation signifies the adsorption of TO molecules onto the internal surface area of pure AC, without causing a shift in the characteristic peaks of AC. It suggests that the TO molecules are more likely physisorbed than chemisorbed on the surface of AC, favoring the physisorption of TO molecules on the AC surface for controlled-release applications of such TO@AC nanohybrids.

Preprints.org (www.preprints.org) | NOT PEER-REVIEWED | Posted: 7 June 2023 doi:10.20944/preprints202306.0500.v1



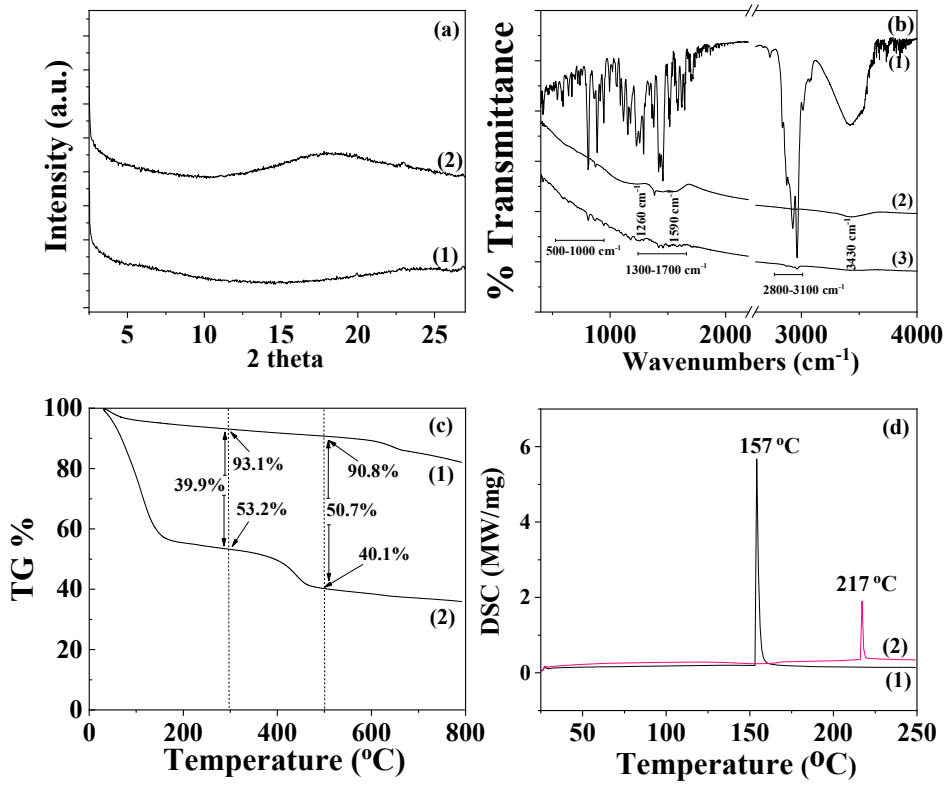


**Figure 4. (a)** XRD plots of (1) pure AC and (2) modified TO@AC nanohybrid in the range of 2 – 30° 2 theta, **(b)** FTIR plots of (1) pure thyme oil, (2) pure AC and (3) modified TO@AC nanohybrid at the range of 400 – 4000 $cm^{-1}$, **(c)** TG plots of (1) pure AC and (2) modified TO@AC nanohybrid in the range of 25 to 800 °C temperature and **(d)** DSC plots of (1) pure AC and (2) modified TO@AC nanohybrid in the range of 0 to 250 °C temperature.

The Thermogravimetric Analysis (TG) plot of pure AC, shown as line (1) in Figure 4c, reveals a mass loss step below 200°C, which aligns with the desorption of AC moisture [53]. The TG plot of AC remains almost unchanged until 600 °C, where a second mass loss step commences [54]. This step correlates with the decomposition of cellulose, lignin, and hemicellulose matter, along with the expulsion of volatile matter that occurs during the carbonization process [55]. The TG plot of the TO@AC nanohybrid (see line (2) in Figure 4c) displays a first mass loss step below 300 °C and a second one beginning at around 350-400 °C and ending around 500 °C. This pattern suggests a fraction of TO desorbs from the AC surface in the temperature range from 150 to 300 °C, while another TO fraction desorbs in a higher temperature range from 350 to 500 °C. Considering the textural features of the AC previously studied [41], the Brünaüer–Emmett–Teller surface area ($S_{gBET}$) of the AC was 1372 $m^2/g$, with the micropore volume being 84.6% and exhibiting micropores at $D_{micro1}$ = 1.28 and $D_{micro2}$ = 1.6 nm [41]. Given that the size of a TO molecule is roughly equal to that of a phenol molecule (about 0.6 – 0.8 nm), a fraction of TO could be adsorbed within the micropore structure of AC. Consequently, the TO fraction residing in the micropores of AC requires more energy to desorb (second mass loss step). It is therefore suggested that the first mass loss step from 150 to 300 °C corresponds to the desorption of TO molecules adsorbed in the mesoporous AC structure, and the second mass loss step from 350 to 500 °C corresponds to the TO molecules desorbed from the microporous AC structure. In Figure 3c, the % mass loss of the first step and the % total mass loss are calculated by subtracting the mass values of TO@AC from the mass values of pure AC at 300 °C and 500 °C respectively. The total TO mass adsorbed is found to be equal to 50.7 wt%, a value considerably higher than those recently obtained for TO adsorption on natural zeolite (35.5 wt%) [40]and HNT (31.4 wt%) [39]. This outcome reveals that AC is a promising bio-based material for application as a nanocarrier in controlled-release applications within the active food packaging

Preprints.org (www.preprints.org) | NOT PEER-REVIEWED | Posted: 7 June 2023 doi:10.20944/preprints202306.0500.v1



sector. The DSC plot of pure AC (see line (1) in Figure 4d) exhibits an exothermic peak at approximately 157 °C, corresponding to the enthalpy of water molecules' desorption. The DSC plot of the modified TO@AC displays a peak around 217°C. This peak aligns more closely with the boiling point of TO (232 °C) than the boiling point of Limonene (176°C), indicating that the fraction of molecules adsorbed in AC is rich in TO molecules, which is consistent with previous publications [39,40]

### *3.2. Physicochemical Characterization of Obtained LDPE/AC and LDPE/TO@AC Films*

#### 3.2.1. XRD Analysis

In Figure 5a the XRD plots of all LDPE/AC and LDPE/TO@AC films as well as pure LDPE film are shown for comparison.

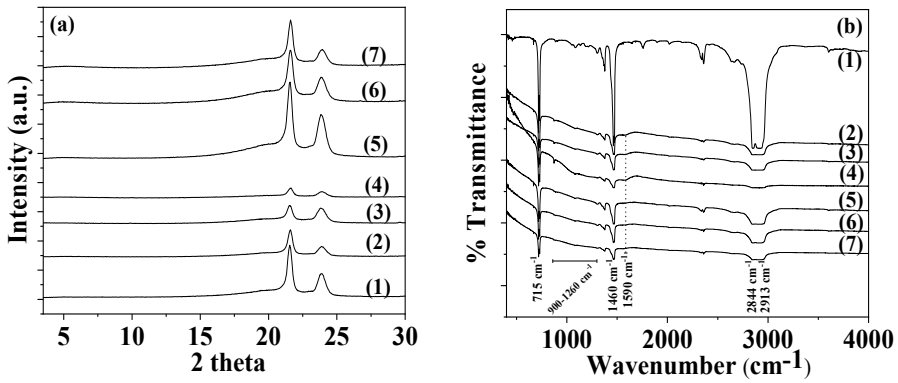


**Figure 5. (a)** XRD plots of pure LDPE and all LDPE/AC and LDPE/TO@AC films, **(b)** FTIR plots of pure LDPE and all LDPE/AC and LDPE/TO@AC films.

In all plots the characteristic peaks of LDPE crystal phase at Bragg angles 2θ1 = 21.5° and 23.75° are observed. It is also observed that by the addition of both AC and TO@AC the LDPE's peaks decreased. In the case of LDPE/AC films the decrease in LDPE's characteristic peaks is higher than in the case of LDPE/TO@AC. This is an indication of higher dispersion of hydrophobic modified TO@AC hybrid in the LDPE matrix than pure AC.

#### 3.2.2. FTIR Spectroscopy

In Figure 5b the FTIR plots of all LDPE/AC and LDPE/TO@AC films as well as pure LDPE film shown for comparison. In all cases the characteristic peaks of LDPE are obtain. More specifically at the bands at 1460 and 715 $cm^{-1}$ are assigned to the asymmetric stretching of the $CH_3$ group, the group wagging of the $CH_2$ group, and the group rocking of the $CH_2$ group of the LDPE. In both LDPE/AC and LDPE/TO@AC films the characteristic peaks of LDPE are decreased and the characteristic peak of AC at 1590 $cm^{-1}$ is obtained as well as the broad peaks of AC in the range of 900 – 1260 $cm^{-1}$. No shift peak of LDPE's characteristic peaks it is observed implying no chemical bonding between LDPE matrix and AC or TO@AC chemical groups [56]. With a more careful glance it is observed that the characteristic peak of AC at 1590 $cm^{-1}$ is more observed in the case of all LDPE/AC films than in the case of LDPE/TO@AC films. This could be an indication of modified and more hydrophobic TO@AC nanohybrid higher dispersion in LDPE matrix than pure AC in accordance with XRD observations hereabove. Finally, no TO peaks are observed in the case of TO@AC containing films and this is an indication that TO molecules are blended inside the LDPE polymer matrix.

Preprints.org (www.preprints.org) | NOT PEER-REVIEWED | Posted: 7 June 2023 doi:10.20944/preprints202306.0500.v1



3.2.3. SEM Images Characterization

The surface/cross-section morphology of the pure polymer matrix LDPE, pure AC and all the obtained LDPE/xAC and LDPE/xTO@AC films were investigated using a SEM instrument and the results confirmed that the AC and hybrid nanostructure TO@AC were homogeneously dispersed in the polymer matrix. The SEM images (surface and cross-section) in Figure 6(a,b) exhibit the expected homogeneous structure of the pristine polymer matrix. In Figure 6(c) the surface morphology of activated carbon (AC) with highly porous characteristics is shown resembling a honeycomb structure. The micro and mesoporous surface morphology in AC acts as an absorbent from the packaged food or as a nanocarrier for bioactive compounds released in the packaged food [57].

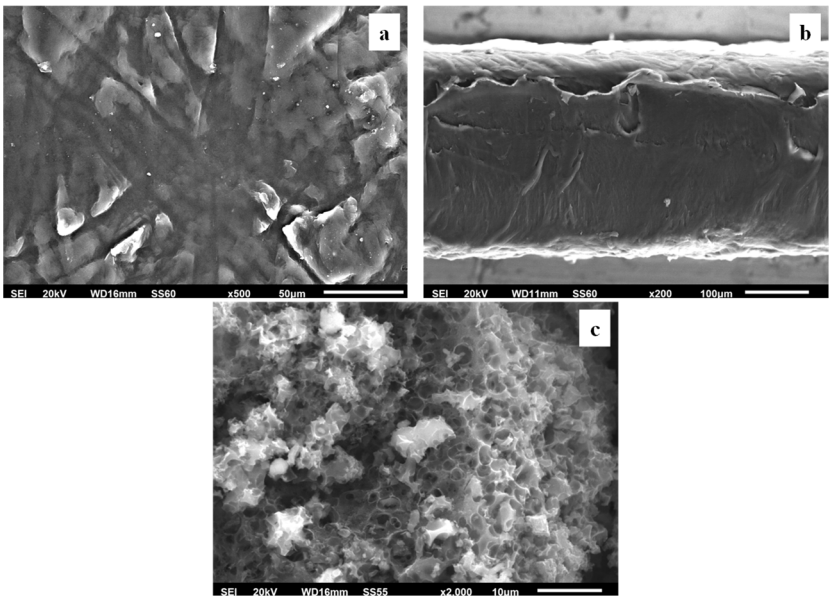


**Figure 6.** (a) SEM images of surface and (b) cross-section for the pure film of LDPE and surface morphology of activated carbon (c).

Surface, relative cross-section images of LDPE/xAC and LDPE/xTO@AC with different ratios (5, 10, 15%) of AC and TO@AC are presented in Figures 7, 8, and 9.

Preprints.org (www.preprints.org) | NOT PEER-REVIEWED | Posted: 7 June 2023 doi:10.20944/preprints202306.0500.v1



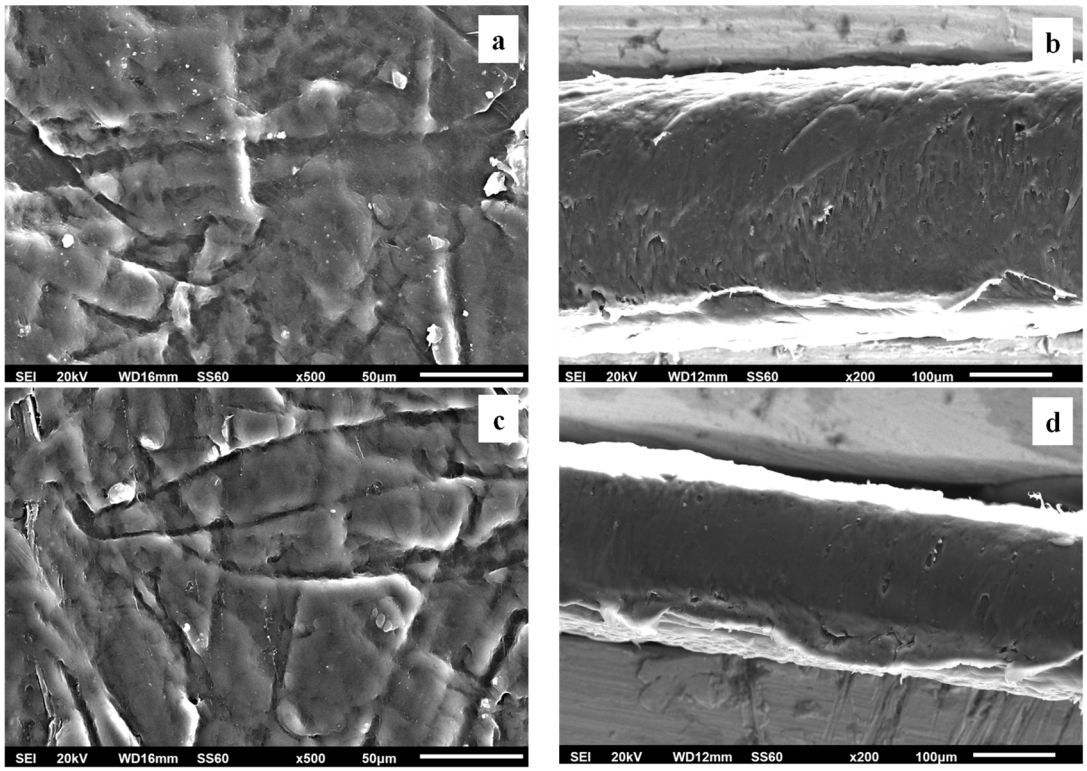


**Figure 7.** (a,c) SEM images of surface and (b,d) cross-section for the nanocomposite films of LDPE/5AC (a,b) and LDPE/5TO@AC (c,d) respectively.

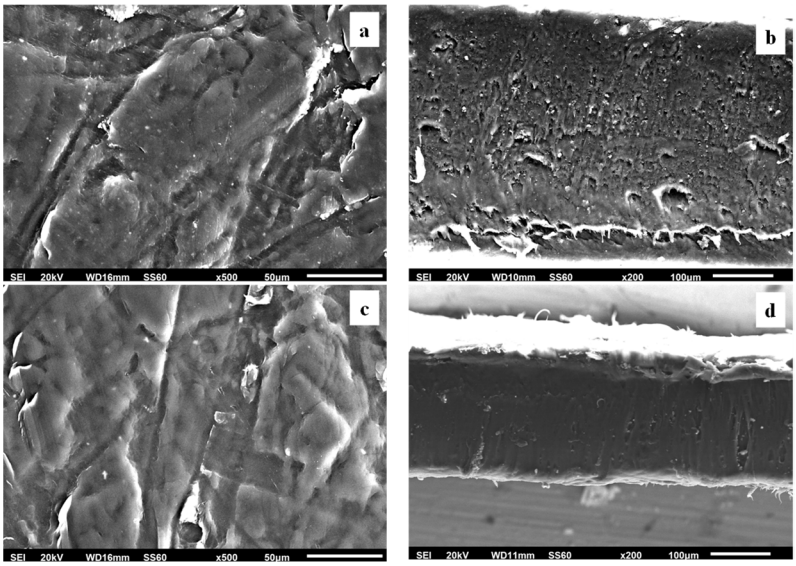


**Figure 8.** (**a,c**) SEM images of surface and (**b,d**) cross-section for the nanocomposite films of LDPE/10AC **(a,b)** and LDPE/10TO@AC **(c,d)** respectively.

Preprints.org (www.preprints.org) | NOT PEER-REVIEWED | Posted: 7 June 2023 doi:10.20944/preprints202306.0500.v1



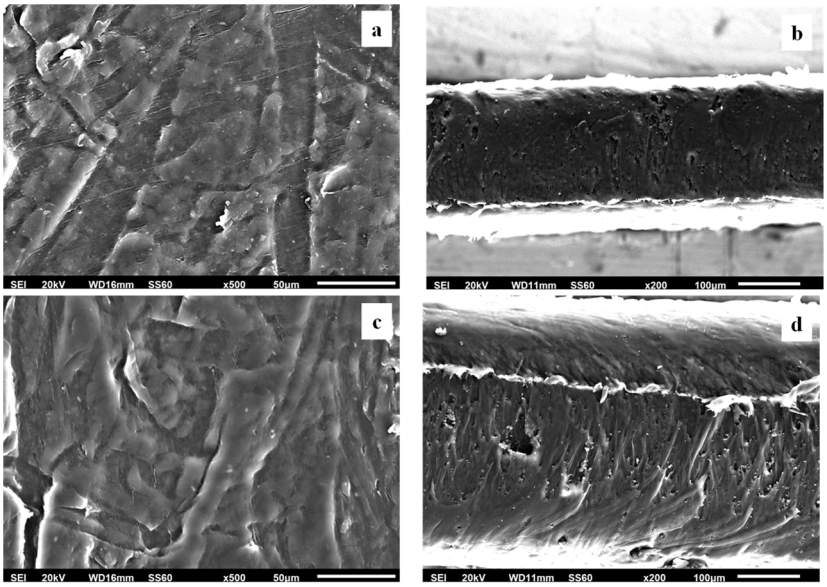


**Figure 9.** (**a,c**) SEM images of surface and (**b,d**) cross-section for the nanocomposite films of LDPE/15AC **(a,b)** and LDPE/15TO@AC (**c,d**) respectively.

Based on the SEM studies it should be mentioned, that in all cases of LDPE/xAC and LDPE/xTO@AC films both AC and TO@AC were homogeneously dispersed indicating their enhanced compatibility and the interfacial adhesion with the polymer matrix of LDPE. This result is combined with XRD and FTIR results discussed hereabove. In advance it is suggested that pure AC derived from spent coffee has a high dispersibility with LDPE matrix due to its hydrophobic nature studied recently [41]. Its hydrophobic nature enhanced by the adsorbed TO molecules and thus enhances more its compatibility with LDPE.

### *3.3. Tensile Properties of LDPE/AC and LDPE/TO@AC Films*

The calculated Elastic Modulus (E), ultimate strength ($\sigma_{uts}$), and elongation at break (%ε) values for all obtained LDPE/AC and LDPE/TO@AC films as well as for pure LDPE film are listed in Table 1 for comparison.

**Table 1.** Elastic Modulus (E), ultimate strength ($\sigma_{uts}$), and elongation at break (%ε) values for all obtained LDPE/AC and LDPE/TO@AC films as well as for pure LDPE film.

| | **E (MPa)** | **$\sigma_{uts}$ (MPa)** | **%ε** |
|---|---|---|---|
| **LDPE** | 183.3±28.8 | 12.6±0.5 | 29.3±8.1 |
| **LDPE/5AC** | 282.7±17.1 | 10.9±1.5 | 33.4±2.7 |
| **LDPE/10AC** | 312.7±21.4 | 11.8±1.9 | 63.4±14.0 |
| **LDPE/15AC** | 327.3±21.8 | 12.7±1.9 | 51.0±12.7 |
| **LDPE/5TO@AC** | 286.0±14.5 | 11.2±1.7 | 43.3±17.5 |
| **LDPE/10TO@AC** | 363.5±19.4 | 12.1±2.4 | 75.8±15.1 |
| **LDPE/15TO@AC** | 291.0±19.0 | 11.8±1.0 | 64.8±18.6 |

As it is obtained in Table 1 incorporation of pure AC powder and modified TO@AC nanohybrid in LDPE matrix do not significantly affect the ultimate strength values of LDPE/AC and LDPE/TO@AC films as compared to the ultimate strength value of pure LDPE film. On the other hand, incorporation of pure AC powder and modified TO@AC nanohybrid in the LDPE increases the Elastic Modulus and % elongation at break values of both LDPE/AC and LDPE/TO@AC films. In

Preprints.org (www.preprints.org) | NOT PEER-REVIEWED | Posted: 7 June 2023 doi:10.20944/preprints202306.0500.v1



advance highest %elongation at break values is obtained for LDPE/TO@AC as compared to the %elongation at break values of LDPE/AC film. The highest %elongation at break values of LDPE/AC films as compared to %elongation at break values of pure LDPE films suggest the high dispersity and compatibility of AC powder in the LDPE matrix. In contrast to our previous reports where inorganic nanostructures such as HNT and NZ have been incorporated in LDPE matrix and lead to fragile LDPE/HNT and LDPE/NZ films the AC powder seems to be more hydrophobic and less inorganic and thus more compatible with LDPE matrix [39,40]. On the contrary with the results present here Sadakpipanich et. al. [36] shown that the incorporation of MC activated carbon into LDPE increased tensile strength and decreased elongation at break of obtained LDPE/MC films. But Sadakpipanich et. al. [36] have incorporated MC contents lower than 5 wt.%. into LDPE films. Thus, herein it is reported for first time that incorporation of high contents of AC varying from 5 to 15% into LDPE into LDPE/AC films with similar or higher elongation at break values in comparison to pure LDPE. It seems that the higher amounts of AC incorporated into LDPE reacts somehow as plasticizer. In advance, the plasticization capacity of AC increased for TO@AC nanohybrids because of the TO molecules presence [12,58,59]. Overall, the highest Elastic Modulus, and % elongation at break values is for LDPE/10TO@AC film. So, this film it is obtained 98.3% and 158.7% highest Elastic Modulus, and % elongation at break values than pure LDPE film correspondingly.

### *3.4. Water and Oxygen Barrier Properties of LDPE/AC and LDPE/TO@AC Films*

In Table 2 the obtained Water vapor transmission rate (WVTR), and oxygen transmission rate (OTR) values of all LDPE/AC and LDPE/TO@AC films as well as for pure LDPE films are listed. From these values the water vapor diffusion coefficient ($D_{wv}$) values and the oxygen permeability ($Pe_{O2}$) values for all LDPE/AC and LDPE/TO@AC films as well as for pure LDPE films were calculated and listed in the Table 2 for comparison.

**Table 2.** Water vapor transmission rate (WVTR), water vapor diffusion coefficient ($D_{wv}$), oxygen transmission rate (OTR) and oxygen permeability ($Pe_{O2}$) values for all LDPE/AC and LDPE/TO@AC films as well as for pure LDPE films.

| | **Film thickness (mm)** | **Water Vapor Transmition Rate ($10^{-7}$ gr.cm$^{-2}$.s$^{1}$)** | **Diffusion Coefficient $D_{wv}$ ($10^{-4}$ cm$^2$/s)** | **Film thickness (mm)** | **Oxygen Transmition Rate (ml.m$^{-2}$.day$^{-1}$)** | **$Pe_{O2}$ ($10^{-8}$cm$^2$/s)** |
|---|---|---|---|---|---|---|
| **LDPE** | 0.270±0.012 | 5.89±0.13 | 3.77±0.17 | 0.270±0.010 | 6407±120 | 20.02±2.41 |
| **LDPE/5AC** | 0.256±0.011 | 6.42±0.56 | 3.73±0.07 | 0.266±0.004 | 1365±62 | 4.19±0.2 |
| **LDPE/10AC** | 0.141±0.014 | 7.31±0.20 | 2.35±0.02 | 0.378±0.010 | 818±15 | 3.57±0.21 |
| **LDPE/15AC** | 0.176±0.010 | 5.02±0.73 | 1.99±0.31 | 0.410±0.015 | 675±34 | 3.20±0.19 |
| **LDPE/5TO@AC** | 0.332±0.012 | 3.96±0.53 | 2.84±0.23 | 0.170±0.015 | 1593±67 | 3.12±0.17 |
| **LDPE/10TO@AC** | 0.186±0.016 | 4.55±0.13 | 1.87±0.21 | 0.311±0.005 | 642±17 | 2.11±0.16 |
| **LDPE/15TO@AC** | 0.241±0.013 | 2.62±0.23 | 1.47±0.04 | 0.351±0.010 | 228±6 | 0.92±0.04 |

As it is obtained in Table 2 both AC powder and TO@AC nanohybrid succeed to increase both water and oxygen barrier. As AC and TO@AC content increase the water and oxygen barrier increases further. A higher water and oxygen barrier increase succeed for TO@AC containing films in accordance with the higher dispersion of LDPE/TO@AC as compared to LDPE/AC films shown in SEM images section here above. So, the lowest water vapor diffusion coefficient ($D_{wv}$) and oxygen permeability ($Pe_{O2}$) values are obtained for LDPE/15TO@AC film. For this film the obtain water vapor diffusion coefficient ($D_{wv}$) value is 55% lowest than the water vapor diffusion coefficient ($D_{wv}$) value of pure LDPE film while its oxygen permeability ($Pe_{O2}$) value is 95.4% lower than the oxygen

Preprints.org (www.preprints.org) | NOT PEER-REVIEWED | Posted: 7 June 2023 doi:10.20944/preprints202306.0500.v1



permeability ($Pe_{O2}$) value of pure LDPE film. Sadakpipanich et. al. [36] developed LDPE based films by incorporating AC produced from biomass derived from macadamia nut cultivation. They findings shows lower water and oxygen barrier properties by varying the AC's wt%. content from 1 to 5%. Therefore, herein it is for first time shown that spent coffee derived AC is a promising material to be applied as a nanoreinforcement to reduce water/oxygen permeability in active packaging films when it is incorporated to LDPE films in high wt% contents from 5 to 15%. Its capacity to increase water/oxygen barrier is maximized when modified with TO to obtain TO@AC nanohybrid.

*3.5. Antioxidant activity of LDPE/TO@AC films*

The plots of % antioxidant activity of all LDPE/TO@AC films as a function of time shown in the Figure 10.

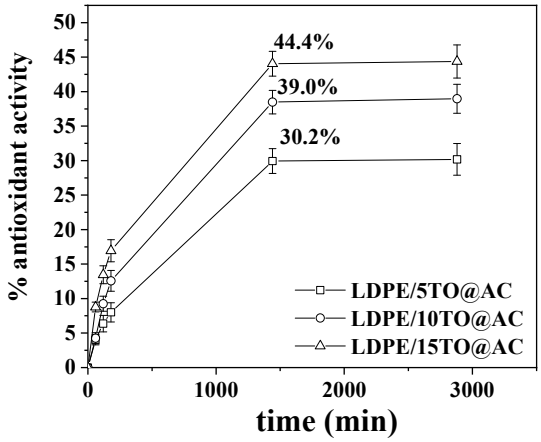


**Figure 10.** Plots of calculated % antioxidant activity of LDPE/5TO@AC, LDPE/10TO@AC, and LDPE/15TO@AC film as a function of time.

As it is obtained in Figure 10 total antioxidant activity of films increases rapidly during the first day and then remains constant. As it is expected antioxidant activity increases as the wt%. TO content in films increases. So, after 1 day incubation LDPE/5TO@AC, LDPE/10TO@AC and LDPE/15TO@AC films reach a total antioxidant activity of 30.2%, 39.0% and 44.4% respectively.

*3.6. TO Release Test - Calculation of Released to wt.% Content and TO Released Diffusion Coefficient ($D_{TO}$) of LDPE/TO@AC Films*

By using the data given in Table S1, S2 and S3 and the equations (2), (3) and (4) the diffusion coefficient of TO released as well as the total amount of TO released ($q_e$) and the desorption rate constant value ($K_2$) for all studied LDPE/xTO@AC films were calculated and are listed in Table 4 for comparison.

**Table 4.** Calculated values of diffusion coefficient of TO molecule, total desorbed amount of TO ($q_e$) and desorption rate constant ($K_2$) for all obtained LDPE/xTO@AC active films.

| | $D_{TO}$ x $10^{-7}$ ($cm^2/s$) | $q_e$ (mg) | $K_2$ |
|---|---|---|---|
| **LDPE/5TO@AC** | 1.39±0.45 | 0.023±0.002 | 2.425±0.419 |
| **LDPE/10TO@AC** | 2.00±0.33 | 0.032±0.006 | 2.444±0.355 |
| **LDPE/15@TOAC** | 1.47±0.86 | 0.044±0.009 | 1.488±0.142 |

Preprints.org (www.preprints.org) | NOT PEER-REVIEWED | Posted: 7 June 2023 doi:10.20944/preprints202306.0500.v1



As it is obtained in Table 4 as the wt.% content of TO@AC used the value of $q_e$ increased and the value of constant $K_2$ decreased. This means the by increasing the content of TO@AC nanohybrid in LDPE/xTO@AC active films the total released TO amount increases and its release rate is lower. On the other hand, the calculated values od TO diffusion coefficient is 1.39 $10^{-7}$ $cm^2/s$ for LDPE/5TO@AC film, 2.00.$10^{-7}$ $cm^2/s$ for LDPE/10TO@AC film and 1.47.$10^{-7}$ $cm^2/s$ for LDPE/15TO@AC film. The values of TO diffusion coefficient and $K_2$ release rate constant reported here and rate are on order of magnitude higher than the TO diffusion coefficient values reported recently for the TO diffusion coefficient and $K_2$ release rate constant from LDPE/xTO@NZ films[40]. This means that AC releases higher amounts of TO and in higher rates than natural zeolite (NZ) [40].

### *3.7. Lipid Oxidation of Pork Fillets*

The calculated TBARS values of the low-fat pork fillets wrapped and packaged with pure LDPE, LDPE/15AC and LDPE/15TO@AC films are shown in Table 5 for comparison. As it is obtained the calculated TBARS values from 0 to 12$^{th}$ day are similar to these recently reported[39,40]. From Table 4 it is obtained that both LDPE/15AC and LDPE/15TO@AC films succeed to reduce obtained TBARS values during the 12 days of storage in comparison to pure LDPE film. In addition, the lowest TBARS values during the 12 days of storage are obtained for LDPE/15TO@AC active film.

**Table 5.** TBARS and Heme-Iron ψontent of pork fillets wrapped with pure LDPE, LDPE/15AC and LDPE/15TOAC films with respect to storage Time.

| | ***Day 0*** | ***Day 2*** | ***Day 4*** | ***Day 6*** | ***Day 8*** | ***Day 10*** | ***Day 12*** |
|---|---|---|---|---|---|---|---|
| **TBARS** | | | | **AVG ± SD (mg/kg)** | | | |
| Control | $0.23^{a} \pm 0.01$ | $0.33^{b} \pm 0.02$ | $0.46^{d} \pm 0.01$ | $0.63^{g} \pm 0.03$ | $0.98^{j} \pm 0.02$ | $1.21^{m} \pm 0.02$ | $1.36^{p} \pm 0.02$ |
| LDPE/15AC | - | $0.28^{b} \pm 0.01$ | $0.40^{e} \pm 0.01$ | $0.53^{h} \pm 0.01$ | $0.83^{k} \pm 0.03$ | $1.10^{n} \pm 0.04$ | $1.28^{q} \pm 0.01$ |
| LDPE/15TO@AC | - | $0.23^{c} \pm 0.01$ | $0.33^{f} \pm 0.02$ | $0.44^{i} \pm 0.02$ | $0.75^{l} \pm 0.03$ | $0.95^{o} \pm 0.03$ | $1.13^{r} \pm 0.02$ |
| | | | | **ANOVA** | | | |
| F | - | 39.577 | 63.033 | 82.765 | 91.031 | 67.336 | 149.763 |
| *p* | - | 0.000 | 0.000 | 0.000 | 0.000 | 0.000 | 0.000 |
| | ***Day 0*** | ***Day 2*** | ***Day 4*** | ***Day 6*** | ***Day 8*** | ***Day 10*** | ***Day 12*** |
| **Fe** | | | | **AVG ± SD (μg/g)** | | | |
| Control | $10.18^{a} \pm 0.12$ | $8.00^{b} \pm 0.12$ | $6.16^{e} \pm 0.12$ | $5.12^{h} \pm 0.19$ | $3.54^{k} \pm 0.16$ | $2.22^{n} \pm 0.27$ | $1.28^{p} \pm 0.15$ |
| LDPE/15AC | - | $8.96^{c} \pm 0.09$ | $6.80^{f} \pm 0.09$ | $5.72^{i} \pm 0.12$ | $4.14^{l} \pm 0.18$ | $2.48^{n} \pm 0.15$ | $1.82^{q} \pm 0.09$ |
| LDPE/15TO@AC | - | $9.66^{d} \pm 0.12$ | $7.92^{g} \pm 0.12$ | $7.40^{j} \pm 0.27$ | $5.70^{m} \pm 0.16$ | $3.84^{o} \pm 0.18$ | $2.48^{r} \pm 0.15$ |
| | | | | **ANOVA** | | | |
| F | - | 162.781 | 186.000 | 99.771 | 135.130 | 52.083 | 60.200 |
| *p* | - | 0.000 | 0.000 | 0.000 | 0.000 | 0.000 | 0.000 |

*Different letters in its column indicate statistically significant differences at the confidence level *p<0.05 (see also Table S4 and S5).*

Preprints.org (www.preprints.org) | NOT PEER-REVIEWED | Posted: 7 June 2023 doi:10.20944/preprints202306.0500.v1



So, in accordance with recent reports [39,40] both LDPE/15AC and LDPE/15TO@AC active films succeed to significantly decrease the deterioration of pork fillets due to the lipid oxidation process.

*3.8. Heme Iron of Pork Fillets*

In the Table 5 are also included the calculated heme iron values. These values as it is expected are decreased for the 12 days of storage for all tested films. The lowest decrease of heme iron values it is obtained for LDPE/15TO@AC film packaged pork fillets. For pork fillets packaged with LDPE/15AC active films heme iron values are higher than LDPE/15TOAC films but lower than pure LDPE films. Thus, both LDPE/15AC and LDPE/15TO@AC films succeed to preserve the pork fillets with higher heme iron contents which is beneficial for nutritional point of view. In advance, in accordance with previous recent reports heme iron contents of pork fillets have a linear correlation with obtained TBARS values [39,40].

*3.9. Correlation of TBARS and Heme Iron*

Throughout storage, the bivariate Pearson's correlation analysis was performed on the obtained TBARS and heme iron content values of pork fillets. The analysis results indicated that significant and positive correlations were observed between the two methods throughout the storage period. The Supplementary Material provides the corresponding correlations (see to Tables S6), which were determined in relation to packaging treatment and storage time.

*3.10. Microbiological Changes of Pork Fillets*

TVC gives a quantitative estimate of the population of microorganisms such as bacteria, yeasts, and molds in a food sample capable of forming visible colonies. Most microorganisms present in pork fillets, either as part of its natural microflora, or as the result of cross contamination from other sources, are mostly aerobic microorganisms and their population is an indicator of product microbiological quality [49]. Table 6 shows the changes in TVC of pork fillets as a function of film used and storage time.

**Table 6.** Total Variable Counts of pork fillets wrapped with pure LDPE, LDPE/15AC and LDPE/15TOAC with respect to storage time.

| | DAYS | | | | |
|---|---|---|---|---|---|
| **Sample name** | **0** | **2** | **4** | **6** | **8** |
| | logCFU/g (Avg ± SD) | | | | |
| LDPE | 3,15±0,06$^{a}$ | 4,56±0,32$^{b}$ | 5,65±0,24$^{d}$ | 6,98±0,41$^{f}$ | 7,88±0,20$^{h}$ |
| LDPE/15AC | 3,15±0,06$^{a}$ | 4,15±0,12$^{c}$ | 5,52±0,18$^{d}$ | 6,68±0,32$^{f}$ | 7,53±0,21$^{h}$ |
| LDPE/15TO@AC | 3,15±0,06$^{a}$ | 3,86±0,09$^{c}$ | 4,53±0,08$^{e}$ | 5,77±0,17$^{g}$ | 6,84±0,14$^{i}$ |
| | ANOVA | | | | |
| F* | - | 8,914 | 35,032 | 11,935 | 28,478 |
| P* | - | 0,0160 | 0,0000 | 0,0080 | 0,0010 |

*Anova results, confidence level p<0,05 (see also Table S7).

As shown in Table 6, the initial value of TVC was 3.15 log cfu/g, indicating a very good microbiological quality of pork meat. According to ICMSF [60] the upper microbiological limit for acceptable quality of foods TVC reached is 7 log cfu/g. This limit value (7 log cfu/g) almost reach for pork fillets wrapped with pure LDPE and LDPE/15AC films on 6$^{th}$ day of storage. For pork fillets wrapped with LDPE/15TO@AC active film, TVC limit value (7 log cfu/g) reached on day 8$^{th}$ day of storage. Thus, it is obvious that TVC values for pork fillets wrapped with pure LDPE and LDPE/15AC films were significantly higher ($p<0.05$) in comparison to pork fillets wrapped with LDPE/15TO@AC active film. In advance, no statistically significant differences ($p>0.05$) were observed for pork fillets

Preprints.org (www.preprints.org) | NOT PEER-REVIEWED | Posted: 7 June 2023 doi:10.20944/preprints202306.0500.v1



wrapped with pure LDPE and LDPE/15AC films. Pork fillets wrapped with LDPE/15AC film shown significantly lower TVC value from pork fillets wrapped with pure LDPE film only on 2nd day of storage. So, it seems that LDPE/15AC film which has a higher oxygen barrier than pure LDPE film succeed to prevent microbiological growth in pork fillets during the first 2 days of storage. For day 2 to day 8 the active LDPE/15TO@AC film succeed to prevent microbiological growth in pork fillets against pure LDPE and LDPE/15AC films due to its ability to release TO in the fillets. Overall, it is concluded that LDPE/15TO@AC active film succeed to extend the microbiological shelf-life of pork fillets by 2 days. Assuming that both LDPE/15AC and LDPE/15TO@AC films have a higher water/oxygen barrier than pure LDPE film it is concluded that TO release is the key factor for extending the shelf – life of wrapped pork fillets.

## 4. Conclusions

In the current study, the preparation and characterization of novel TO@AC nanohybrids, the development and characterization of innovative LDPE/TO@AC active packaging films, and their application in pork fillets preservation were studied in detail. Here are the most innovative points of this study:

As demonstrated, the hydrophobic AC derived from spent coffee proved to be an excellent nanocarrier for essential oils components such as TO, yielding TO@AC nanohybrids with high amounts (50 wt.%) of TO physiosorbed in mesoporous and microporous of AC.

The high quantity of physiosorbed TO molecules on AC resulted in LDPE/xTO@AC films with higher TO release rates than the TO release rates recently referred to for similar LDPE active films with TO molecules adsorbed in natural zeolite (NZ) nanofiller.

XRD, FTIR results, and SEM images demonstrated that both pure AC and TO@AC exhibit excellent dispersity and compatibility with the LDPE matrix. This high dispersity allowed the development of LDPE/xAC and LDPE/xTO@AC films with wt.% amounts of AC and TO@AC used up to 15 wt.%, a first in this field. The high dispersity of both pure AC and TO@AC nanohybrid in LDPE resulted in LDPE/xAC and LDPE/xTO@AC films having superior elongation-at-break values and improved water/oxygen barrier properties compared to pure LDPE film.

In general, LDPE/xTO@AC films exhibited greater elongation-at-break values and superior water/oxygen barrier properties due to the presence of TO molecules. LDPE/xTO@AC active films also showed significant antioxidant activity.

The film with the highest barrier properties and greatest antioxidant activity was used as packaging film for pork fillet preservation. Pure LDPE and LDPE/15AC films were also used as packaging films for pork fillets for comparison. The monitoring of TBARS lipid oxidation values, heme iron values, and TVC values of packaged pork fillets during 12 days of storage concluded that the LDPE/15TO@AC film had the lowest TVC and TBARS values, and the highest heme iron values compared to pure LDPE and LDPE/15AC over the 12-day storage period.

The LDPE/15TO@AC active film could potentially extend the microbiological shelf-life of pork fillets by 2 days.

**Supplementary Materials:** The following supporting information can be downloaded at the website of this paper posted on Preprints.org.

**Author Contributions:** Synthesis experiment design, A.E.G. and C.E.S.; characterization measurements and interpretation, A.E.G., V.I.K., A.L., I.K.K., D.M., A.K-M., N.A., A.A.; G. K.; S,G., and C.E.S.; paper writing, A.E.G., and C.E.S.; V.I.K., A.L., overall evaluation of this work, A.E.G. and C.E.S.; experimental data analysis and interpretation, A.E.G., V.I.K., A.A., I.K.K., D.M., A.A., M.B., S,G., G. K.; C. P.; and C.E.S.; XRD, OTR, tensile measurements, antioxidant activity, WVTR experimental measurements, Release Kinetics test V.I.K; A.E.G. and C.E.S, and pork fillets shelf life packaging test V.I.K., A.L., K.Z., I.K.K., N.A., S,G., G. K.; and A.E.G., SEM images D. M., A.K-M., A. A.; FTIR analysis, A.E.G.; C. E. S. All authors have read and agreed to the published version of the manuscript.

**Acknowledgments:** Authors want to thank the meat processing company Aifantis Company (Aifantis Group – Head Quarters, Acheloos Bridge, Agrinio, Greece 30100, e-Mail: info@aifantis.gr , website: www.aifantis-group.com/ ) for the kind offer of “skalopini type” fresh pork fillets.

Preprints.org (www.preprints.org) | NOT PEER-REVIEWED | Posted: 7 June 2023 doi:10.20944/preprints202306.0500.v1



**Data Availability Statement:** The datasets generated for this study are available on request to the corresponding author.

**Conflicts of Interest:** The authors declare no conflict of interest.

## References


1. Ahmed, Md.W.; Haque, Md.A.; Mohibbullah, Md.; Khan, Md.S.I.; Islam, M.A.; Mondal, Md.H.T.; Ahmmed, R. A Review on Active Packaging for Quality and Safety of Foods: Current Trends, Applications, Prospects and Challenges. *Food Packaging and Shelf Life* **2022**, *33*, 100913, doi:10.1016/j.fpsl.2022.100913.
2. Soltani Firouz, M.; Mohi-Alden, K.; Omid, M. A Critical Review on Intelligent and Active Packaging in the Food Industry: Research and Development. *Food Research International* **2021**, *141*, 110113, doi:10.1016/j.foodres.2021.110113.
3. Yildirim, S.; Röcker, B.; Pettersen, M.K.; Nilsen-Nygaard, J.; Ayhan, Z.; Rutkaite, R.; Radusin, T.; Suminska, P.; Marcos, B.; Coma, V. Active Packaging Applications for Food. *Comprehensive Reviews in Food Science and Food Safety* **2018**, *17*, 165–199, doi:10.1111/1541-4337.12322.
4. Carocho, M.; Morales, P.; Ferreira, I.C.F.R. Natural Food Additives: Quo Vadis? *Trends in Food Science & Technology* **2015**, *45*, 284–295, doi:10.1016/j.tifs.2015.06.007.
5. Saltmarsh, M. Recent Trends in the Use of Food Additives in the United Kingdom. *Journal of the Science of Food and Agriculture* **2015**, *95*, 649–652, doi:10.1002/jsfa.6715.
6. Almeida-Souza, F.; Magalhães, I.F.B.; Guedes, A.C.; Santana, V.M.; Teles, A.M.; Mouchrek, A.N.; Calabrese, K.S.; Abreu-Silva, A.L. Safety Assessment of Essential Oil as a Food Ingredient. In *Essential Oils: Applications and Trends in Food Science and Technology*; Santana de Oliveira, M., Ed.; Springer International Publishing: Cham, 2022; pp. 123–171 ISBN 978-3-030-99476-1.
7. Carpena, M.; Nuñez-Estevez, B.; Soria-Lopez, A.; Garcia-Oliveira, P.; Prieto, M.A. Essential Oils and Their Application on Active Packaging Systems: A Review. *Resources* **2021**, *10*, 7, doi:10.3390/resources10010007.
8. Essential Oils in Food Preservation, Flavor and Safety - 1st Edition Available online: https://www.elsevier.com/books/essential-oils-in-food-preservation-flavor-and-safety/preedy/978-0-12-416641-7 (accessed on 11 January 2023).
9. Coşkun, B.K.; Çalikoğlu, E.; Emiroğlu, Z.K.; Candoğan, K. Antioxidant Active Packaging with Soy Edible Films and Oregano or Thyme Essential Oils for Oxidative Stability of Ground Beef Patties. *Journal of Food Quality* **2014**, *37*, 203–212, doi:10.1111/jfq.12089.
10. Hosseini, S.F.; Zandi, M.; Rezaei, M.; Farahmandghavi, F. Two-Step Method for Encapsulation of Oregano Essential Oil in Chitosan Nanoparticles: Preparation, Characterization and in Vitro Release Study. *Carbohydrate Polymers* **2013**, *95*, 50–56, doi:10.1016/j.carbpol.2013.02.031.
11. Wang, L.; Liu, T.; Liu, L.; Liu, Y.; Wu, X. Impacts of Chitosan Nanoemulsions with Thymol or Thyme Essential Oil on Volatile Compounds and Microbial Diversity of Refrigerated Pork Meat. *Meat Science* **2022**, *185*, 108706, doi:10.1016/j.meatsci.2021.108706.
12. Giannakas, A.E.; Salmas, C.E.; Leontiou, A.; Baikousi, M.; Moschovas, D.; Asimakopoulos, G.; Zafeiropoulos, N.E.; Avgeropoulos, A. Synthesis of a Novel Chitosan/Basil Oil Blend and Development of Novel Low Density Poly Ethylene/Chitosan/Basil Oil Active Packaging Films Following a Melt-Extrusion Process for Enhancing Chicken Breast Fillets Shelf-Life. *Molecules* **2021**, *26*, 1585, doi:10.3390/molecules26061585.
13. Salmas, C.E.; Giannakas, A.E.; Baikousi, M.; Leontiou, A.; Siasou, Z.; Karakassides, M.A. Development of Poly(L-Lactic Acid)/Chitosan/Basil Oil Active Packaging Films via a Melt-Extrusion Process Using Novel Chitosan/Basil Oil Blends. *Processes* **2021**, *9*, 88, doi:10.3390/pr9010088.
14. Chaiwarit, T.; Ruksiriwanich, W.; Jantanasakulwong, K.; Jantrawut, P. Use of Orange Oil Loaded Pectin Films as Antibacterial Material for Food Packaging. *Polymers* **2018**, *10*, 1144, doi:10.3390/polym10101144.
15. Yang, H.-J.; Song, K.B. Application of Lemongrass Oil-Containing Polylactic Acid Films to the Packaging of Pork Sausages. *Korean J Food Sci Anim Resour* **2016**, *36*, 421–426, doi:10.5851/kosfa.2016.36.3.421.
16. Sivaram, S.; Somanathan, H.; Kumaresan, S.M.; Muthuraman, M.S. The Beneficial Role of Plant Based Thymol in Food Packaging Application: A Comprehensive Review. *Applied Food Research* **2022**, *2*, 100214, doi:10.1016/j.afres.2022.100214.
17. Ochoa-Velasco, C.E.; Pérez-Pérez, J.C.; Varillas-Torres, J.M.; Navarro-Cruz, A.R.; Hernández-Carranza, P.; Munguía-Pérez, R.; Cid-Pérez, T.S.; Avila-Sosa, R. Starch Edible Films/Coatings Added with Carvacrol and Thymol: In Vitro and In Vivo Evaluation against Colletotrichum Gloeosporioides. *Foods* **2021**, *10*, 175, doi:10.3390/foods10010175.
18. Srisa, A.; Harnkarnsujarit, N. Antifungal Films from Trans-Cinnamaldehyde Incorporated Poly(Lactic Acid) and Poly(Butylene Adipate-Co-Terephthalate) for Bread Packaging. *Food Chemistry* **2020**, *333*, 127537, doi:10.1016/j.foodchem.2020.127537.
19. Arrieta, M.P.; López, J.; Ferrándiz, S.; Peltzer, M.A. Characterization of PLA-Limonene Blends for Food Packaging Applications. *Polymer Testing* **2013**, *32*, 760–768, doi:10.1016/j.polymertesting.2013.03.016.

Preprints.org (www.preprints.org) | NOT PEER-REVIEWED | Posted: 7 June 2023 doi:10.20944/preprints202306.0500.v1




20. Giannakas, E.A.; Leontion, A. Montmorillonite Composite Materials and Food Packaging. *Packaging Materials* **2018**, 1–71.
21. Giannakas Na-Montmorillonite Vs. Organically Modified Montmorillonite as Essential Oil Nanocarriers for Melt-Extruded Low-Density Poly-Ethylene Nanocomposite Active Packaging Films with a Controllable and Long-Life Antioxidant Activity. *Nanomaterials* **2020**, *10*, 1027, doi:10.3390/nano10061027.
22. Giannakas, A.E.; Salmas, C.E.; Karydis-Messinis, A.; Moschovas, D.; Kollia, E.; Tsigkou, V.; Proestos, C.; Avgeropoulos, A.; Zafeiropoulos, N.E. Nanoclay and Polystyrene Type Efficiency on the Development of Polystyrene/Montmorillonite/Oregano Oil Antioxidant Active Packaging Nanocomposite Films. *Applied Sciences* **2021**, *11*, 9364, doi:10.3390/app11209364.
23. Giannakas, A.E.; Salmas, C.E.; Leontiou, A.; Moschovas, D.; Baikousi, M.; Kollia, E.; Tsigkou, V.; Karakassides, A.; Avgeropoulos, A.; Proestos, C. Performance of Thyme Oil@Na-Montmorillonite and Thyme Oil@Organo-Modified Montmorillonite Nanostructures on the Development of Melt-Extruded Poly-L-Lactic Acid Antioxidant Active Packaging Films. *Molecules* **2022**, *27*, 1231, doi:10.3390/molecules27041231.
24. Saucedo-Zuñiga, J.N.; Sánchez-Valdes, S.; Ramírez-Vargas, E.; Guillen, L.; Ramos-deValle, L.F.; Graciano-Verdugo, A.; Uribe-Calderón, J.A.; Valera-Zaragoza, M.; Lozano-Ramírez, T.; Rodríguez-González, J.A.; et al. Controlled Release of Essential Oils Using Laminar Nanoclay and Porous Halloysite / Essential Oil Composites in a Multilayer Film Reservoir. *Microporous and Mesoporous Materials* **2021**, *316*, 110882, doi:10.1016/j.micromeso.2021.110882.
25. de Oliveira, L.H.; Trigueiro, P.; Souza, J.S.N.; de Carvalho, M.S.; Osajima, J.A.; da Silva-Filho, E.C.; Fonseca, M.G. Montmorillonite with Essential Oils as Antimicrobial Agents, Packaging, Repellents, and Insecticides: An Overview. *Colloids and Surfaces B: Biointerfaces* **2022**, *209*, 112186, doi:10.1016/j.colsurfb.2021.112186.
26. Blinka, T.A.; Edwards, F.B.; Miranda, N.R.; Speer, D.V.; Thomas, J.A. Zeolite in Packaging Film 1997.
27. de Araújo, L.O.; Anaya, K.; Pergher, S.B.C. Synthesis of Antimicrobial Films Based on Low-Density Polyethylene (LDPE) and Zeolite A Containing Silver. *Coatings* **2019**, *9*, 786, doi:10.3390/coatings9120786.
28. Dogan, H.; Koral, M.; İnan, T.Y. Ag/Zn Zeolite Containing Antibacterial Coating for Food-Packaging Substrates. *Journal of Plastic Film & Sheeting* **2009**, *25*, 207–220, doi:10.1177/8756087909354479.
29. Gargiulo, N.; Attianese, I.; Buonocore, G.G.; Caputo, D.; Lavorgna, M.; Mensitieri, G.; Lavorgna, M. $\alpha$-Tocopherol Release from Active Polymer Films Loaded with Functionalized SBA-15 Mesoporous Silica. *Microporous and Mesoporous Materials* **2013**, *167*, 10–15, doi:10.1016/j.micromeso.2012.07.037.
30. Khezri, K.; Roghani-Mamaqani, H. Effect of MCM-41 Nanoparticles on ARGET ATRP of Styrene: Investigating Thermal Properties Available online: https://journals.sagepub.com/doi/abs/10.1177/0021998314535961?journalCode=jcma (accessed on 20 November 2019).
31. Chaemsanit, S.; Matan, N.; Matan, N. Activated Carbon for Food Packaging Application: Review. *Walailak Journal of Science and Technology (WJST)* **2018**, *15*, 255–271, doi:10.48048/wjst.2018.4185.
32. Sobhan, A.; Muthukumarappan, K.; Wei, L.; Van Den Top, T.; Zhou, R. Development of an Activated Carbon-Based Nanocomposite Film with Antibacterial Property for Smart Food Packaging. *Materials Today Communications* **2020**, *23*, 101124, doi:10.1016/j.mtcomm.2020.101124.
33. Mitura, K.; Kornacka, J.; Kopczyńska, E.; Kalisz, J.; Czerwińska, E.; Affeltowicz, M.; Kaczorowski, W.; Kolesińska, B.; Frączyk, J.; Bakalova, T.; et al. Active Carbon-Based Nanomaterials in Food Packaging. *Coatings* **2021**, *11*, 161, doi:10.3390/coatings11020161.
34. Idrees, M.; Rangari, V.; Jeelani, S. Sustainable Packaging Waste-Derived Activated Carbon for Carbon Dioxide Capture. *Journal of CO2 Utilization* **2018**, *26*, 380–387, doi:10.1016/j.jcou.2018.05.016.
35. Pomponio, L.; Ruiz-Carrascal, J. Oxidative Deterioration of Pork during Superchilling Storage. *Journal of the Science of Food and Agriculture* **2017**, *97*, 5211–5215, doi:10.1002/jsfa.8403.
36. Sakdapipanich, J.; Rodgerd, P.; Sakdapipanich, N. A Low-Density Polyethylene (LDPE)/Macca Carbon Advanced Composite Film with Functional Properties for Packaging Materials. *Polymers* **2022**, *14*, 1794, doi:10.3390/polym14091794.
37. Giannakas, A.E.; Salmas, C.E.; Moschovas, D.; Zaharioudakis, K.; Georgopoulos, S.; Asimakopoulos, G.; Aktypis, A.; Proestos, C.; Karakassides, A.; Avgeropoulos, A.; et al. The Increase of Soft Cheese Shelf-Life Packaged with Edible Films Based on Novel Hybrid Nanostructures. *Gels* **2022**, *8*, 539, doi:10.3390/gels8090539.
38. Constantinos E. Salmas; Aris E. Giannakas; Dimitrios Moschovas; Eleni Kollia; Stsvros Georgopoulos; Christina Gioti; Areti Leontiou; Apostolos Avgeropoulos; Anna Kopsacheili; Learda Avdulai; et al. Kiwi Fruits Preservation Using Novel Edible Active Coatings Based on Rich in Thymol Halloysite Nanostructures and Chitosan/Polyvinyl Alcohol Gels. *Gels Bioactive Gel Films and Coatings Applied in Active Food Packaging*.
39. Giannakas, A.E.; Salmas, C.E.; Moschovas, D.; Karabagias, V.K.; Karabagias, I.K.; Baikousi, M.; Georgopoulos, S.; Leontiou, A.; Katerinopoulou, K.; Zafeiropoulos, N.E.; et al. Development, Characterization, and Evaluation as Food Active Packaging of Low-Density-Polyethylene-Based Films

Preprints.org (www.preprints.org) | NOT PEER-REVIEWED | Posted: 7 June 2023 doi:10.20944/preprints202306.0500.v1



Incorporated with Rich in Thymol Halloysite Nanohybrid for Fresh "Scaloppini" Type Pork Meat Fillets Preservation. *Polymers* **2023**, *15*, 282, doi:10.3390/polym15020282.
40. Salmas, C.E.; Giannakas, A.E.; Karabagias, V.K.; Moschovas, D.; Karabagias, I.K.; Gioti, C.; Georgopoulos, S.; Leontiou, A.; Kehayias, G.; Avgeropoulos, A.; et al. Development and Evaluation of a Novel-Thymol@Natural-Zeolite/Low-Density-Polyethylene Active Packaging Film: Applications for Pork Fillets Preservation. *Antioxidants* **2023**, *12*, 523, doi:10.3390/antiox12020523.
41. Asimakopoulos, G.; Baikousi, M.; Kostas, V.; Papantoniou, M.; Bourlinos, A.B.; Zbořil, R.; Karakassides, M.A.; Salmas, C.E. Nanoporous Activated Carbon Derived via Pyrolysis Process of Spent Coffee: Structural Characterization. Investigation of Its Use for Hexavalent Chromium Removal. *Applied Sciences* **2020**, *10*, 8812, doi:10.3390/app10248812.
42. Giannakas, A.; Giannakas, A.; Ladavos, A. Preparation and Characterization of Polystyrene/Organolaponite Nanocomposites. *Polymer - Plastics Technology and Engineering* **2012**, *51*, doi:10.1080/03602559.2012.704115.
43. Giannakas, A.E.; Salmas, C.E.; Moschovas, D.; Baikousi, M.; Kollia, E.; Tsigkou, V.; Karakassides, A.; Leontiou, A.; Kehayias, G.; Avgeropoulos, A.; et al. Nanocomposite Film Development Based on Chitosan/Polyvinyl Alcohol Using ZnO@Montmorillonite and ZnO@Halloysite Hybrid Nanostructures for Active Food Packaging Applications. *Nanomaterials* **2022**, *12*, 1843, doi:10.3390/nano12111843.
44. Giannakas, A.; Stathopoulou, P.; Tsiamis, G.; Salmas, C. The Effect of Different Preparation Methods on the Development of Chitosan/Thyme Oil/Montmorillonite Nanocomposite Active Packaging Films. *Journal of Food Processing and Preservation* **2019**.
45. Salmas, C.E.; Giannakas, A.E.; Baikousi, M.; Kollia, E.; Tsigkou, V.; Proestos, C. Effect of Copper and Titanium-Exchanged Montmorillonite Nanostructures on the Packaging Performance of Chitosan/Poly-Vinyl-Alcohol-Based Active Packaging Nanocomposite Films. *Foods* **2021**, *10*, 3038, doi:10.3390/foods10123038.
46. Tarladgis, B.G.; Watts, B.M.; Younathan, M.T.; Dugan, L. A Distillation Method for the Quantitative Determination of Malonaldehyde in Rancid Foods. *J Am Oil Chem Soc* **1960**, *37*, 44–48, doi:10.1007/BF02630824.
47. Karabagias, I.; Badeka, A.; Kontominas, M.G. Shelf Life Extension of Lamb Meat Using Thyme or Oregano Essential Oils and Modified Atmosphere Packaging. *Meat Science* **2011**, *88*, 109–116, doi:10.1016/j.meatsci.2010.12.010.
48. Clark, E.M.; Mahoney, A.W.; Carpenter, C.E. Heme and Total Iron in Ready-to-Eat Chicken. *J. Agric. Food Chem.* **1997**, *45*, 124–126, doi:10.1021/jf960054l.
49. Assanti, E.; Karabagias, V.K.; Karabagias, I.K.; Badeka, A.; Kontominas, M.G. Shelf Life Evaluation of Fresh Chicken Burgers Based on the Combination of Chitosan Dip and Vacuum Packaging under Refrigerated Storage. *J Food Sci Technol* **2021**, *58*, 870–883, doi:10.1007/s13197-020-04601-4.
50. Darvish, M.; Ajji, A. Synergistic Antimicrobial Activities of Limonene with Mineral Carriers in LDPE Films for Active Packaging Application. *Science Journal of Chemistry* **2022**, *10*, 32, doi:10.11648/j.sjc.20221002.11.
51. Salmas, C.E.; Giannakas, A.E.; Moschovas, D.; Kollia, E.; Georgopoulos, S.; Gioti, C.; Leontiou, A.; Avgeropoulos, A.; Kopsacheili, A.; Avdylaj, L.; et al. Kiwi Fruits Preservation Using Novel Edible Active Coatings Based on Rich Thymol Halloysite Nanostructures and Chitosan/Polyvinyl Alcohol Gels. *Gels* **2022**, *8*, 823, doi:10.3390/gels8120823.
52. Yakout, S.M.; Sharaf El-Deen, G. Characterization of Activated Carbon Prepared by Phosphoric Acid Activation of Olive Stones. *Arabian Journal of Chemistry* **2016**, *9*, S1155–S1162, doi:10.1016/j.arabjc.2011.12.002.
53. Pathak, U.; Jhunjhunwala, A.; Roy, A.; Das, P.; Kumar, T.; Mandal, T. Efficacy of Spent Tea Waste as Chemically Impregnated Adsorbent Involving Ortho-Phosphoric and Sulphuric Acid for Abatement of Aqueous Phenol—Isotherm, Kinetics and Artificial Neural Network Modelling. *Environ Sci Pollut Res* **2020**, *27*, 20629–20647, doi:10.1007/s11356-019-06014-z.
54. *Activated Carbon Adsorption*; CRC Press, 2005; ISBN 978-0-429-11418-2.
55. Hadoun, H.; Sadaoui, Z.; Souami, N.; Sahel, D.; Toumert, I. Characterization of Mesoporous Carbon Prepared from Date Stems by H3PO4 Chemical Activation. *Applied Surface Science* **2013**, *280*, 1–7, doi:10.1016/j.apsusc.2013.04.054.
56. Giannakas, A.; Salmas, C.; Leontiou, A.; Tsimogiannis, D.; Oreopoulou, A.; Braouhli, J. Novel LDPE/Chitosan Rosemary and Melissa Extract Nanostructured Active Packaging Films. *Nanomaterials* **2019**, *9*, 1105, doi:10.3390/nano9081105.
57. Moosavi, S.; Lai, C.W.; Gan, S.; Zamiri, G.; Akbarzadeh Pivehzhani, O.; Johan, M.R. Application of Efficient Magnetic Particles and Activated Carbon for Dye Removal from Wastewater. *ACS Omega* **2020**, *5*, 20684–20697, doi:10.1021/acsomega.0c01905.
58. Zubair, M.; Shahzad, S.; Hussain, A.; Pradhan, R.A.; Arshad, M.; Ullah, A. Current Trends in the Utilization of Essential Oils for Polysaccharide- and Protein-Derived Food Packaging Materials. *Polymers* **2022**, *14*, 1146, doi:10.3390/polym14061146.

Preprints.org (www.preprints.org) | NOT PEER-REVIEWED | Posted: 7 June 2023 doi:10.20944/preprints202306.0500.v1



59. Aitboulahsen, M.; El Galiou, O.; Laglaoui, A.; Bakkali, M.; Hassani Zerrouk, M. Effect of Plasticizer Type and Essential Oils on Mechanical, Physicochemical, and Antimicrobial Characteristics of Gelatin, Starch, and Pectin-Based Films. *Journal of Food Processing and Preservation* **2020**, *44*, e14480, doi:10.1111/jfpp.14480.
60. Stewart, G.S.A.B. Micro-Organisms in Food—2. Sampling for Microbiological Analysis: Principles and Specific Applications: ICMSF, Blackwell Scientific Publications, Oxford, 1986. 310 Pp. Price: £19·50 (Cloth). *Meat Science* **1987**, *19*, 315, doi:10.1016/0309-1740(87)90078-7.

**Disclaimer/Publisher's Note:** The statements, opinions and data contained in all publications are solely those of the individual author(s) and contributor(s) and not of MDPI and/or the editor(s). MDPI and/or the editor(s) disclaim responsibility for any injury to people or property resulting from any ideas, methods, instructions or products referred to in the content.